Cannabinoids Activate the Insulin Pathway to Modulate Mobilization of Cholesterol in *C. elegans*

Short Title

Endocannabinoids and cholesterol mobilization

Authors

Bruno Hernandez-Cravero[1], Sofia Gallino[2], Jeremy Florman[3], Cecilia Vranych[1], Philippe Diaz[4], Ana Belén Elgoyhen[2], Mark J. Alkema[3] and Diego de Mendoza[1]*

Affiliations

[1]Laboratorio de Fisiología Microbiana, Instituto de Biología Molecular y Celular de Rosario (IBR), CONICET, Facultad de Ciencias Bioquímicas y Farmacéuticas, Universidad Nacional de Rosario, 2000, Rosario, Argentina.

[2]Laboratorio de Fisiología y Genética de la Audición, Instituto de Investigaciones en Ingeniería Genética y Biología Molecular "Dr. Héctor N. Torres" (INGEBI), Consejo Nacional de Investigaciones Científicas y Técnicas (CONICET), Buenos Aires, Argentina.

[3]Department of Neurobiology, University of Massachusetts Medical School, Worcester, MA, USA.

[4]Department of Biomedical and Pharmaceutical Sciences, University of Montana, 32 Campus Drive, Missoula, Montana 59812, USA

*Corresponding author

Contact information for corresponding author

Diego de Mendoza

Instituto de Biología Molecular y Celular de Rosario (IBR, CONICET-UNR), 2000EXF Rosario, Argentina

Electronic address: demendoza@ibr-conicet.gov.ar

Keywords

C. elegans, endocannabinoid, genetic analysis, cholesterol, RNAi enhancer screen insulin pathway

Abstract

The nematode *Caenorhabditis elegans* requires exogenous cholesterol to survive and its depletion leads to early development arrest. Thus, tight regulation of cholesterol storage and distribution within the organism is critical. Previously, we demonstrated that the endocannabinoid (eCB) 2-arachidonoylglycerol (2-AG) plays a key role in *C. elegans* modulating sterol mobilization, but the mechanism is unknown. Here we show that mutations in the *ocr-2* and *osm-9* genes coding for transient receptors potential V (TRPV) ion channels, dramatically reduces the effect of 2-AG in cholesterol mobilization. Through genetic analysis combined with the rescuing of larval arrest induced by sterol starvation we found that the insulin/IGF-1signaling (IIS) pathway and UNC-31/CAPS, a calcium-activated regulator of neural dense-core vesicles release, are essential for 2-AG-mediated stimulation of cholesterol mobilization. These findings indicate that 2-AG-dependent cholesterol trafficking requires the release of insulin peptides and signaling through the DAF-2 insulin receptor. These results suggest that 2-AG acts as an endogenous modulator of TRPV signal transduction to control intracellular sterol traffic through modulation of the IGF-1 signaling pathway.

Author summary

Although cannabis extracts have been used in folklore medicine for centuries, the past few years have seen an increased interest in the medicinal uses of cannabinoids, the bioactive components of the cannabis plant, for treatment of many diseases of the nervous system. However, the human body naturally produces endocannabinoids that are similar to the cannabinoids present in Cannabis sativa. Our goal is to understand how endocannabinoids maintain cholesterol homeostasis in animals, underscoring the importance of cholesterol balance for healthy life. Both cholesterol excess and cholesterol deficiency can have detrimental effects on health, and a myriad of regulatory processes have thus evolved to control the metabolic pathways of sterol metabolism. The nematode *C. elegans* is auxotroph for sterols, that is; contrary to mammals they cannot synthesize sterols, therefore, dietary supply is essential for survival. The aim of our study was to elucidate the mechanism by which endocannabinoids abolish larval arrest of *C. elegans* induced by cholesterol depletion. We discovered that endocannabinoids stimulate the insulin pathway, which affects development, reproduction and life span, to modulate mobilization of cholesterol in *C. elegans*. Our studies have important implications for a better understanding of human pathological conditions associated with impaired cholesterol homeostasis.

Introduction

Cholesterol is essential for a diverse range of cellular processes, including hormone signaling, fat metabolism, and membrane structure and dynamics. Dysregulation of cholesterol and lipid homeostasis can have a major impact on development and disease [1,2]. Cholesterol deficiency can result in blunted steroid hormone production, reduced serotonin levels, vitamin deficiencies, and increased mortality, whereas cholesterol excess is a risk factor for cardiovascular disease, diabetes, neurodegeneration, and inflammation [3–8]. Thus, understanding cholesterol and lipid homeostasis is critical to illuminate aspects of human health and longevity.

The nematode *Caenorhabditis elegans* requires exogenous cholesterol because cannot synthesize it de novo [9]. In *C. elegans*, cholesterol regulates at least two processes. First, it is required for growth and progression through larval stages, as well as for proper shedding of old cuticles during larval molting events [10]. Second, it regulates entry into a specialized diapause stage adapted for survival under harsh conditions, called the dauer larva [11]. Tight spatial and temporal regulation of uptake, storage, and transport of sterols to appropriate subcellular compartments is required for cholesterol to exert its diverse cellular functions [10].

Despite the pivotal role of sterols in *C. elegans* development, the regulation of cholesterol metabolism is only now beginning to be understood. Previously, it was shown that worms grown in the absence of cholesterol arrest as dauer-like larvae in the second generation [9]. The sterols that govern dauer formation are bile-acid-like hormones called dafachronic acids (DAs) [11]. Molecular mechanisms underlying their function have been intensely studied. DAs inhibit dauer formation by binding to the

nuclear hormone receptor DAF-12, which, in the absence of DAs, activates the dauer program [12,13]. Even though cholesterol is associated with cell membranes and interacts with multiple lipid species, very little is known about how lipids influence cholesterol trafficking. It was recently discovered that the *C. elegans* glycolipids, phosphoethanolamine glucosylceramides (PEGCs), stimulates the growth of worms by a yet unknown mechanism under conditions of cholesterol scarcity [14]. We also recently reported that the best studied endocannabinoids (eCBs) 2-arachidonoyl glycerol (2-AG) and arachidonoyl ethanolamine (AEA), which are lipid messengers that elicit a plethora of biological functions in mammals, enhance traffic of cholesterol in *C. elegans* [15]. We found that these eCBs stimulate worm growth under conditions of cholesterol scarcity and reverse the developmental arrest of *ncr-1-2* mutants [15]. *ncr-1* and *ncr-2* encode proteins with homology to the human Niemann-Pick type C (NP-C) disease gene (*NPC-1*) and are involved in the intracellular cholesterol trafficking in *C. elegans* [16]. The mechanism by which these signaling lipids exert their effects on cholesterol homeostasis within large endocrine networks is unknown. Here we show that 2-AG promotes cholesterol mobilization through pathways that are independent of known *C. elegans* cannabinoid-like receptors that mediates regulation of regenerative axon navigation [17] and behavior [18]. We find that mutations in the ocr-2 and osm-9 genes coding for transient receptors potential of the vanilloid subtype (TRPV), ion channels, dramatically reduces the effect of 2-AG in cholesterol mobilization. We also find that the insulin/IGF 1 signaling (IIS) pathway and UNC-31/CAPS, the calcium-activated regulator of dense-core vesicles exocytosis (DCVs), are necessary for 2-AG-mediated stimulation of cholesterol mobilization. This suggests that 2-AG-dependent cholesterol traffic requires signaling of insulin peptides through the DAF-2 insulin receptor. Our results indicate that

118 2-AG acts as endogenous modulators of TRPV channels to control intracellular sterol

119 traffic through modulation of the insulin/IGF-1 (IIS) signaling pathway.

120

Results

FAAH-4 is involved in cholesterol homeostasis in *C. elegans.*

C. elegans interrupts reproductive development and arrest as L2-like larvae when grown for two generations without cholesterol [9]. Previously, we have found that this arrest is abolished by supplementation with the eCB 2-AG [15, Fig.1A]. Recent work has revealed that the monoacylglycerol lipase FAAH-4, but not other FAAH enzymes in *C. elegans*, hydrolyzes 2-AG [19]. To test the specificity of eCB signaling we asked whether a *faah-4* deletion (*⊿faah-4*) could enhance the rescuing effect of 2-AG on the arrest induced by cholesterol depletion in *C. elegans*. Indeed, we found that under sterol free conditions exogenous 2-AG (50 µM) significantly increases the formation of adults in *⊿faah-4* animals compared to wild-type animals (Fig 1A). In agreement with this result, *faah-4* animals displayed elevated levels of endogenous 2-AG compared to the wild type (Fig. 1B, [19]). Next, we investigated whether a *faah-4* deficiency relieves the phenotype of mutations that perturb cholesterol transport. We found that FAAH-4 RNAi decreased the Daf-c penetrance in null mutants for the Niemann-Pick homologues *ncr-1-2* (Fig 1C). As expected, FAAH-4 RNAi also enhanced the ability of a low concentration of 2-AG (10 µM) to suppress dauer formation of *ncr-1-2* double mutants (Fig 1C). These results confirm the specificity of 2-AG in cholesterol mobilization and suggest that FAAH-4 is an important enzyme in cholesterol homeostasis.

2-AG controls cholesterol homeostasis through NPR-19 and NPR-32 independent pathways

The biological effect of 2-AG in mammals are mediated through its interaction with the G -protein coupled type-1 (CB1) and type-2 (CB2) cannabinoid receptors [20–22]. In a study comparing of vertebrate CB1 to other G protein-coupled receptors (GPCRs) in the *C. elegans* genome, two neuropeptide receptors (NPRs), NPR-19 and NPR-32, were shown to have conservation of the critical amino acid residues involved in eCB ligand binding [17]. NPR-19 has been shown to be a 2-AG receptor that modulates monoaminergic (e.g., serotonin and dopamine) signaling in *C. elegans* [18]. To determine whether NPR-19 is required for the 2-AG-mediated stimulation of cholesterol mobilization, we screened the mutant animals for loss of 2-AG-dependent enhancement of cholesterol trafficking. In particular, we tested the interaction of NPR-19 with the DAF-7/TGF-β pathway, which plays an important role in promoting development by affecting cholesterol metabolism and DA production [14]. *daf-7* mutants constitutively form dauer larvae when grown in normal dietary cholesterol (13 µM) due to impaired cholesterol trafficking [14]. We found that *npr-19* did not increase the penetrance of Daf-C defects seen in *daf-7* mutants at 20°C (Fig 2A). Moreover, dauer formation in both *daf-7* and *daf-7*; *npr-19* mutant animals were rescued by either 2-AG or 2-arachidonoylglycerol-eter (2-AGE) (Fig 2A), a non-hydrolysable analog of 2-AG. In agreement with this prediction, 2-AG relieved the dauer arrest of *npr-19* and npr-32 mutants when cholesterol was depleted from the diet (0 µg/ml) (Fig 2B), indicating that 2-AG stimulation of cholesterol trafficking is independent of NPR-19 and NPR-32. Moreover, 2-AG rescued the arrest of the double mutant *npr-19*; *npr-32* under cholesterol depletion, ruling out the possibility that these two receptors might

167 redundantly act in the eCB effect. Together, these data demonstrate that 2-AG acts in
168 cholesterol mobilization through NPR-19 and NPR-32 independent pathways. We also
169 tested several 2-AG candidates, such as GPCRs and neurotransmitter receptors,
170 identified by examination of protein BLAST data using human CB1 receptors. However,
171 we found that animals mutated in these potential targets were rescued by 2-AG, under
172 cholesterol depletion (S1 Table).

173 **TRPV channels are required for 2-AG-dependent cholesterol mobilization**

174 In mammals many cannabinoids can activate transient receptor potential vanilloid
175 (TRPV) channels [23]. *ocr-2* encodes a channel of the TRPV subfamily that functions in *C.*
176 *elegans* olfaction, nociception and osmosensation [24]. We found that, similarly to *C.*
177 *elegans fat-3* and *fat-4* mutants, which are deficient in PUFAs and display aberrant
178 cholesterol mobilization [15], *ocr-2* animals displayed a high incidence of arrested larvae
179 in the first generation without cholesterol (Fig 3A and 3B). While 2-AG suppresses dauer
180 formation of *fat* mutants [15], 2-AG was unable to rescue the arrest of *ocr-2* animals
181 starved from cholesterol. To determine the specificity of *ocr-2* requirement for
182 mobilization of cholesterol, we examined mutants for other TRPV channels. The *C.*
183 *elegans* genome encodes five members of the TRPV family, *ocr-1* through *ocr-4* and *osm-*
184 *9*. We found that null mutations in *ocr-1, ocr-3* and *ocr-4* produced almost 100% gravid
185 adults in the first generation without cholesterol. In contrast, about 50% of the *osm-9*
186 animals starved of cholesterol exhibited a dauer-like phenotype in the first generation,
187 similar to in *ocr-2* mutants. 2-AG was also unable to prevent the arrest of *osm-9* animals
188 starved from cholesterol (Fig 3A). Together, these data demonstrate that both *osm-9*
189 and *ocr-2* mutations eliminate 2-AG-dependent cholesterol mobilization.

In *C. elegans*, both, *osm-9* and *ocr-2* TRPV genes are expressed in the ADF serotonergic neurons and also co-expressed in five pairs of non-serotonergic chemosensory neurons: the AWA, ADL, ASH neurons in the head, and the PHA and PHB neurons in the tail [25]. It has been reported that OSM-9 and OCR-2, regulate in ADF, 5-HT biosynthesis through the modulation of the *tph-1* gene expression, which encodes a key enzyme required for 5-HT biosynthesis from tryptophan [26]. A recent report suggested that 2-AG stimulates 5-HT release through a pathway requiring OSM-9, from the serotonergic ADF neurons to modulate *C. elegans* behavior [27]. However, we found that the ability of 2-AG to rescue the development of cholesterol depleted worms is unaffected by mutations in *tph-1* or in mutants in 5-HT receptors (S1 Fig and S1 Table). These results indicate that 2-AG stimulation of cholesterol mobilization in *C. elegans* is independent of 5-HT release.

Both OSM-9 and OCR-2 are thought to function cooperatively and assemble into homo- and hetero-tetramers [28]. Recent electrophysiological studies employing a *Xenopus laevis* oocyte expression system demonstrated that OSM-9/OCR-2 respond to warming, suggesting that these channels cooperatively function as a temperature receptor [29]. Because OSM-9 and OCR-2 channels mediate influx of divalent cations with a preference for calcium [30], we hypothesized that 2-AG is an agonist of channels containing OSM-9 and/or OCR-2 subunits and that activation of the channel is the trigger mechanism for 2-AG-induced mobilization of cholesterol in *C. elegans*. To test this hypothesis, we expressed OSM-9 and OCR-2 in *Xenopus* oocytes and recorded current Two-electrode voltage clamp. Our analysis showed that 2-AG did not elicit currents in *Xenopus* oocytes injected with *osm-9* and *ocr-2* cRNA either alone or in combination (S2 Fig). However,

warm stimulus (about 36 ºC) evoked currents in *Xenopus* oocytes simultaneous injected with both *osm-9* and *ocr-2* cRNA (S2 Fig), indicating that the channel was active.

To determine whether 2-AG can induce neuronal activity in vivo in neurons that co-express *osm-9* and *ocr-2* we used calcium imaging. 100 µM 2-AG failed to induce calcium transients in animal that express the GCaMP6 in the ASH neurons (S3 Fig). Since 2-AG did not induce OSM-9/OCR-2 channel activation in vitro or in vivo, it suggests that this compound acts upstream or in parallel of TRPV channels in sensory transduction.

The cannabinoid based T-Type calcium channel blocker NMP331 antagonizes the action of 2-AG on cholesterol mobilization.

Since the effect of 2-AG on cholesterol mobilization appears not to be mediated by CB receptors orthologues (Fig 2), we tested synthetic cannabinoid ligands with the expectation that some of these compounds may act as inverse agonist/antagonist of 2-AG. This approach has been used to identify lipophilic molecules that interact with putative eCB receptors with conserved function but diverge from canonical mammalian receptors [31]. We reasoned that if a synthetic ligand blocks a cannabinoid signaling pathway involved in cholesterol trafficking, the Daf-c defects seen in *daf-7* mutants would be increased. We tested whether a series of CB1/CB2 receptor ligands (NMP compounds) that target both CB receptors and T-type calcium channels [32,33] modulate Daf-c phenotype of *daf-7* (e1372) mutants. Of the four compounds tested, only one compound, NMP331 (named as compound 10 in reference 33), at a concentration of 1µM robustly enhanced the dauer phenotype of *daf-7* at semi-permissive temperature (20°C) (Fig 4A). Supplementation of growth media with an excess of cholesterol lowered dauer formation in *daf-7* exposed to NMP331 (Fig 4B),

suggesting that this compound affects sterol mobilization. If NMP331 affects cholesterol mobilization, we predicted that wild-type animals in the presence of this compound would arrest already in the first generation without externally provided sterols. While wild type animals, produced almost 100% gravid adults in the first generation without cholesterol, exposure to NMP331 in the absence of cholesterol resulted in a high incidence (20%) of arrested larvae with typical dauer morphology (Fig 4C and S4A Fig). Furthermore, 2-AG antagonizes the enhancing effect of 1 µM of NMP331 on dauer formation in *daf-7* worms in a dose-response manner (S4B Fig), suggesting that NMP331 acts in the same pathway or in parallel to 2-AG.

Strikingly, when *fat-4* animals which are unable to synthesize AEA or 2-AG [15] were exposed to NMP331 in a cholesterol depleted medium formed 90% dauers in the first generation, while untreated animals produced mostly gravid adults (Fig 4C).

Using radio-ligand assays and electrophysiology in human embryonic kidney cells, it was determined that compound NMP331 in addition to show high affinity for CB1 receptors is also a blocker of the CaV3.2 T-type calcium channel [33]. Unlike vertebrates that possess three genes that encode T-calcium channels, the genome of *C. elegans* encodes a single T-type channel named *cca-1* [34]. We found that 2-AG-dependent cholesterol mobilization was still present in a *cca-1* mutant (Fig 4D), suggesting that this T-type channel is not the target of NMP331 antagonizing the 2-AG effect in *C. elegans.*

Taken together we conclude that NMP331 impacts cholesterol availability, transport and/or metabolism by antagonizing the stimulatory role of 2-AG in cholesterol mobilization. At this point we do not know whether NMP331 affects other molecular

targets, such as ion channels, involved in the cannabinoid-mediated modulation of cholesterol trafficking.

SBP-1 is required for 2-AG modulation of cholesterol mobilization

To identify potential *C. elegans* genes controlling the regulatory circuit of 2-AG-mediated cholesterol mobilization, we performed RNAi enhancer screen on *daf-7* temperature sensitive mutants, using an RNAi library containing transcriptions factors, transporters and nuclear receptors potentially involved in cholesterol homeostasis (S2 Table). We first surveyed for enhancement of the *daf-7* Daf-c phenotype and, in a secondary survey, screened for loss of 2-AG-dependent rescue of the developmental arrest caused by cholesterol depletion.

We identified two loci, *nhr-8* and *sbp-1*, that in combination with *daf-7* give a strong Daf-c constitutive phenotype (S2 Table). *nhr-8*, codes for a nuclear receptor that plays an important role in cholesterol homeostasis in *C. elegans* [35], while *sbp-1*, encodes the single orthologue of the sterol regulatory element (SREBP) family which regulate transcription of genes required to many aspects of lipid metabolism [36]. We found that supplementation with 2-AG rescued the developmental arrest of *nhr-8* animals depleted of cholesterol (Fig 5A). Thus, *nhr-8* is not positioned within the 2-AG pathway of cholesterol mobilization. In contrast, 2-AG was unable to abolish the developmental arrest induced by cholesterol depletion in *sbp-1(ep79)* animals (Fig 5B). This suggests that 2-AG promotes mobilization of cholesterol, through a pathway requiring the transcriptional activity of SBP-1/SREBP. Consistent with this result, 2-AG was unable to suppress dauer formation in *ncr-1-2* mutants exposed to *sbp-1* RNAi, even though this Daf-c phenotype was largely suppressed by raising the cholesterol concentration in the

281 growth media (Fig 5C). Surprisingly, this high cholesterol concentration did not rescue
282 the Daf-c phenotype of *ncr-1-2* mutants subjected to *sbp-1* RNAi. This suggests that *sbp-*
283 *1* genetically interacts with the Niemann Pick proteins to regulate intracellular
284 cholesterol trafficking. Finally, we found that *sbp-1* animals displayed elevated 2-AG
285 levels compared with control animals (Fig 5D). This could be due to a compensatory
286 mechanism to optimize cholesterol trafficking in animals depleted of SBP-1.

287 Taken together, our results suggest that SBP-1 in concert with the Niemann-Pick
288 homologs plays an important role in the 2-AG signal transduction pathway to mobilize
289 cholesterol.

290 **Mobilization of sterols by 2-AG is controlled by the insulin pathway**

291 The DAF-2/IIS and DAF-7/TGF-β signaling comprise the major endocrine pathways
292 modulating the conversion of cholesterol into DA [13]. In a previous study it was shown
293 that temperature-sensitive *daf-7* mutants are hypersensitive to cholesterol depletion
294 and form dauer larvae in the absence of external cholesterol already at 20˚C [14]. More
295 recently, we reported that upon cholesterol deprivation 2-AG rescues the dauer arrest
296 of *daf-7* animals [15]. We determined that 2-AG also prevents dauer formation in
297 mutants which are defective in core components of the DAF-7/TGF-β signaling pathway
298 (S5A Fig), suggesting that 2-AG functions independently of this pathway.

299 Interestingly, *daf-2(e-1370)* mutants with reduced Insulin-IGF-1 receptor signaling also
300 form about 90% dauers at 20˚C in the first generation in the absence of cholesterol (S.
301 Penkov and T. Kurzchalia, unpublished results). Nevertheless, unlike *daf-7* mutants, 2-
302 AG could not suppress the dauer arrest of *daf-2* animals starved from cholesterol a 20°C
303 (Fig 6A). This suggests that 2-AG-mediated mobilization of cholesterol depends on the

IIS pathway. We also tested the requirement of phosphoinositide-3 kinase AGE-1/PI3K or the serine threonine kinase AKT-1 that act downstream of the DAF-2 insulin receptor. 2-AG was unable to suppress the dauer formation of both single mutants growing under sterol depleted conditions (Fig 6B-C). Finally, we found that the 2-AG antagonist, NMP331, does not enhance the Daf-c phenotype at 20ºC of *daf-2(e1370)* mutants (S5B Fig). This result show that NMP331 requires a functional IIS signaling pathway for its effect on cholesterol trafficking. Taken together, our results suggest that IIS and 2-AG converge in a process essential for cholesterol mobilization.

UNC-31 and HID-1 are required for 2-AG-dependent cholesterol mobilization

We next sought to determine whether 2-AG rescued dauer formation in worms deficient in proteins that act upstream DAF-2, such as UNC-64/syntaxin [37] and UNC-31/CAPS [38]. *unc-64* and *unc-31* mutants have constitutive dauer formation at 27°C but not 25°C (Fig 6D) [39]. Dauer formation of *unc-64* mutant animals was markedly suppressed at 27°C by either 2-AG or DA under normally dietary cholesterol. As expected, high concentrations of cholesterol also suppressed dauer formation of *unc-64* mutants at 27°C (Fig 6D). In contrast, 2-AG was unable to suppress the Daf-c phenotype of *unc-31* mutants, suggesting that its gene product is essential for the 2-AG-dependent mobilization of cholesterol (Fig 6D). Consistent with a role of UNC-31 in cholesterol homeostasis, we found that DA rescues the dauer arrest of *unc-31* animals (Fig 6D). *unc-31* encodes the *C. elegans* homolog of mammalian Ca^{2+} activated protein for secretion (CAPS), required for the regulated release of dense core vesicles (DCVs), which contain biogenic amines, neuropeptide, and insulins [38,40–42]. In addition, 2-AG was unable to rescue the Daf-c phenotype at 27°C of animals deficient in HID-1, a key component in

the secretion of DCVs [43] (S6A Fig). HID-1 is expressed in all neuron and gut cells of *C. elegans*. Expression of HID-1 under the *rab-3* promoter in neurons in a *hid-1(sa722)* mutant background was sufficient to partially restore the rescuing effect of 2-AG on dauer formation (S6B Fig). In contrast, 2-AG failed to rescue dauer formation when HID-1 was expressed under the *ges-1* promoter in the gut of *hid-1* animals (S6B Fig). Taken together, these experiments indicate that diminished neural release of DCVs impairs the effect of 2-AG on cholesterol mobilization.

Discussion

Although cannabis extracts have been used in folklore medicine for centuries, the past few years have increased interest in the medicinal use of cannabinoids, the bioactive components of the cannabis plant for treatment of many diseases of the nervous system. We have recently demonstrated that 2-AG and AEA, the best characterized eCBs reversed the blockade of intracellular trafficking of cholesterol in *C. elegans* [15]. Clearly, unraveling the molecular basis of cholesterol mobilization by eCBs in *C. elegans* could have important implications for a greater understanding of human pathological conditions associated with impaired cholesterol homeostasis. The endogenous cannabinoid 2-AG and AEA are synthesized within the brain and CNS [44]. Cannabinoids primarily activate $G_{\alpha o}$-coupled cannabinoid receptors 1 and 2 (CB1 and CB2)[20,22]. CB1 is localized primarily in the brain and CNS, whereas CB2 is restricted to the periphery and certain leukocytes [45]. Although initial reports suggested that nematodes lacked a canonical CB receptor [46,47], it has been determined that *C. elegans* also possesses cannabinoid-like receptors [17,18]. NPR-19 is a functional orthologue to the mammalian CB1/2, and NPR-32, a functional orthologue to GPR18 and GPR55 [17]. Here we show that the modulation of cholesterol homeostasis by 2-AG is independent of the GPCRs NPR-19 and NPR-32 signaling. Instead, we found that 2-AG displays interactions with components of the insulin/IGF1 signaling, a major endocrine pathway modulating DA production and dauer formation. We determined that reduction of the IIS pathway by mutations in the insulin/IGF receptor homolog *daf-2*, the phosphoinositide-3 kinase AGE-1/PI3K or the serine threonine kinase AKT-1 result in animals that are not rescued by 2-AG in a cholesterol depleted medium (Fig. 6). Since reduction of DAF-2/IIS pathway activity affects significantly 2-AG signaling, we asked whether insulin like peptide

359 secretion control eCB-mediated cholesterol homeostasis. We found that the calcium-
360 activated regulator of dense-core vesicle release (DCVs), UNC-31/CAPS, which functions
361 in the nervous system to mediate release of insulin like peptides [38,40–42] is essential
362 for 2-AG-mediated stimulation of cholesterol mobilization. This result combined with
363 the requirement of *hid-1* for 2-AG signaling suggests that neural release of DCVs is
364 required for 2-AG regulation of cholesterol homeostasis. We hypothesize that 2-AG
365 stimulates cholesterol mobilization through the release of insulin-like peptides.

366 In agreement with early results [9] we have determined that after two generations of
367 cholesterol depletion, DAF-16::GFP fusion protein exhibited significantly higher
368 accumulation in the nucleus than did worms grown on cholesterol supplemented media
369 (Fig 7A and S7 Fig). Exogenous 2-AG largely inhibited the nuclear localization of DAF-16
370 (Fig 7A), adding important evidence that the eCB stimulates the mobilization of
371 cholesterol and its conversion into DA. Once synthesized, DA binds to DAF-12 and in
372 target tissues liganded DAF-12 releases DAF-16 from the nucleus promoting
373 reproductive growth and inhibiting dauer programs [9].

374 The simplest model consistent with previous [15] and present results is that 2-AG has a
375 dual role, promoting the release of insulin peptides contained in DCVs and removing
376 cholesterol from internal pools (Fig 7B). It is not known how and where worms store
377 the internal sterol pools. Even though cholesterol is associated with cell membranes
378 and interacts with multiple lipid species, very little is known about how lipids influence
379 cholesterol trafficking. One of the few examples is the positive effect of the phospholipid
380 lysobisphosphatidic acid on the trafficking of cholesterol through the endolysosomal
381 compartment [48]. Owing to the huge diversity of membrane lipids, multiple other lipid

382 species might emerge as additional modulators of the cholesterol trafficking process.
383 eCBs are amphiphilic molecules derived from phospholipids that are unlikely to diffuse
384 passively in the membrane. Several reports have shown that cholesterol behaves as a
385 specific binding partner for eCBs [49,50]. Following an initial interaction of either 2-AG
386 or AEA with cholesterol, mediated by the establishment of hydrogen bonds, they are
387 attracted towards the membrane interior forming a molecular complex [49,50]. This
388 raises the possibility that the interaction of 2-AG with cholesterol enhances the
389 intracellular trafficking of sterols to steroidogenic tissues, positively affecting production
390 of DAs. This regulated transport of cholesterol demands energy [51]. As upregulation of
391 the insulin pathway is linked to increased metabolic rates [52], 2-AG-mediated
392 activation of the DAF-2 pathway may induce a metabolic shift to provide the fuel needed
393 to meet the high energy demands of *C. elegans* cholesterol mobilization (Fig 7B). In
394 addition, stimulation of the IIS pathway should enforce, together with DA-bound DAF-
395 12, the DAF-16/FOXO nuclear export to rescue the arrest of cholesterol depleted worms
396 (Fig 7B).

397 Many of the physiological effects produced by eCBs are not completely understood. As
398 we report here, some of them may reflect their influence on cholesterol trafficking.
399 Interestingly, eCBs and eCB agonists are known to increase the hepatic expression of
400 SREBP in mice [53]. Here we show that the simple orthologue of mammalian SREBP in
401 *C. elegans*, SBP-1, plays an important role in 2-AG mobilization of cholesterol (Fig. 5B).
402 Notably, RNAi of SBP-1 increases the penetrance of Daf-c defects seen in *daf-2 (e1370*)
403 when grown in normal dietary cholesterol (S8 Fig). Although experimental evidence has
404 demonstrated that *daf-2* controls the expression of numerous genes predicted to
405 participate in fatty acid metabolism [54], it is not clear how DAF-2 and its regulatory

406 targets regulates lipid metabolism. Our findings indicate that SBP-1 and IIS converge on
407 a critical physiological process potentially related to the role of eCBs in cholesterol
408 availability (Fig 7B). Future work should elucidate the nature of such interaction.

409 The specific molecular mechanisms through which *C. elegans* sensory neurons detect
410 eCBs remain to be deciphered, however our findings suggest a key role for the *osm-9*
411 and *ocr-2* TRPV genes in the control of cholesterol trafficking mediated by 2-AG. We
412 found that both *osm-9* and *ocr-2* arrest already in the first generation without externally
413 provided sterols (Fig 3), reminiscent of *fat-3* and *fat-4* mutants which are aberrant in
414 cholesterol mobilization because they are unable to synthesize AEA and 2-AG [15].
415 Moreover, the arrest of *osm-9* and *ocr-2* mutants is not rescued by 2-AG, strongly
416 suggesting that OSM-9/OCR-2 TRPV channel is essential for 2-AG-dependent cholesterol
417 mobilization. Since the TRPV family encodes for non-selective cation channels with a
418 preference for Ca^{2+} [30], it is possible that that OCR-2/OSM-9 may directly activate
419 insulin secretion trough UNC-31, a Ca^{2+} dependent regulator of DCVs release.

420 Although the exact mode of activation of OSM-9 and OCR-2 in neurons is partly
421 understood, our data are consistent with the hypothesis that 2-AG acts upstream of the
422 TRPV channel. Interestingly, it has been suggested that G-protein-coupled lipid signaling
423 pathways regulate TRPV channel signaling in chemosensory neurons [55]. This yet to be
424 identified pathway could be specific inhibited by the cannabinoid based calcium blocker
425 NMP331, that potently competes with 2-AG in cholesterol mobilization (S4B Fig).

426 Our insights in the role of eCBs in nematode cholesterol homeostasis has added an
427 important new piece of information. Yet, the puzzle remains incomplete, and many
428 mechanistic questions have yet to be answered. It seems plausible that both worms and

mammals possess a fully functional eCB signaling pathway that regulates cholesterol homeostasis. Further dissecting cannabinoid regulation of lipid homeostasis in the context of larger endocrine networks should reveal how these processes alter disease states, health and possibly longevity.

Materials and Methods

Materials. 2-AG and 2-AGE were purchased from Cayman Chemical (Ann Arbor, Michigan, USA) and stock solutions are in acetonitrile at 1 mg/ml and are stored at -80 ºC. Cholesterol, Dubelcco´s medium (DMEM) and antioxidant BHT were purchased from Sigma (Sigma-Aldrich, St. Louis, Missouri, USA). Δ4-DA and Δ7-DA were provided by Prof. H.-J. Knölker. All buffers, salts and chemical were reagent grade and were used without further treatments. Unless specified, all reagents were purchased from Merck or Sigma. The cannabinoid receptor ligands (NMP compounds) 241, 242, and 243 are named as compounds 40, 54 and 41 in reference 32. Compound NMP331 is named as compound 10 in reference 33.

Nematode maintenance and strains

Standard *C. elegans* culture and molecular biology methods were used. Strains were cultured at 15°C or 20ºC on nematode growth media (NGM) agar plates with the *E. coli* OP 50 strain as a food source [56]. The wild type strain was Bristol N2. Some strains were provided by the *Caenorhabditis* Genetics Center (CGC) at the University of Minnesota. The strains *hid-1 (sa722), hid-1 (sa722); lin-15 (n765); jsEx897 [rab-3p-HID-1-GFP], hid-1 (sa722); lin-15 (n765); jsEx909 [ges-1p-HID-1-GFP], hid-1 (sa722); lin-15 (n765); jsEx896 [hid-1p-HID-1-GFP] were* kindly provided by D. Rayes. The strains used were: N2 Bristol (wild-type), *daf-7(e1372), daf-2(e1370), daf-2(e1368), fat-4 (ok958), ncr-1 (nr2022); ncr-2 (nr2023), npr-19 (ok2068), tyra-3(ok325), ckr-2(tm3082), gar-2(ok520), gar-3(vu78), gar-1(ok755), ser-2(ok2103), npr-11 (ok594), ser-1(ok345), ser-5(ok3087), npr-5(ok1583), dop-1(vs101) , mod-1(ok103) , octr-1(ok371), npr-16(ok1541), ser-7(tm1325), ser-4(ok512), dop-2(vs105), npr-24(ok312) , dop-1(ok398), npr-32(ok2541),*

npr-35 (ok3258), gnrr-1 (ok238), age-1 (hx546), akt-1 (ok525), daf-4 (e1364), *daf-8* (e1393), *unc-64 (e246), unc-31(e928), daf-14 (m77), daf-28 (sa191), faah-4 (lt121), sbp-1 (ep79), nhr-8 (ok186), ocr-1 (ok132), ocr-2 (ok1711), ocr-3 (ok1559), ocr-4 (vs137), osm-9 (ok1677), daf-11 (m47), tph-1 (mg280), daf-36 (k114), cca-1 (ok3442), zIs356 [daf-16p::daf-16a/b::GFP + rol-6(su1006)]. hid-1 (sa722), hid-1 (sa722); lin-15 (n765); jsEx897 [rab-3p-HID-1-GFP], hid-1 (sa722); lin-15 (n765); jsEx909 [ges-1p-HID-1-GFP], hid-1 (sa722); lin-15 (n765); jsEx896 [hid-1p-HID-1-GFP]; xuEx1978 [Psra-6::Gcamp6(f), Psra-6::DsRed].*

Preparation of sterol-depleted plates and sterol-deprived worm culture.

To obtain sterol-free conditions, agar was replaced by ultrapure agarose and peptone was omitted from plates as described earlier [15]. Briefly, agarose was washed three times overnight with chloroform to deplete the trace sterols in it. Salt composition was kept identical to NGM plates. As a food source, *E. coli* NA22 grown overnight in sterol-free culture medium DMEM was used. Bacteria were rinsed with M9 buffer and 20 times concentrated. Bleached embryos were grown for one generation on sterol-free agarose plates. The resulting gravid adults were bleached and the obtained embryos were used in various assays.

Generation of *daf-7; npr-19* and *npr-19;npr-32* double mutants.

The *daf-7* and *npr-32* mutants were each crossed into *npr-19* to generate double mutants by standard methods. Crosses were confirmed by PCR genotyping and constitutive dauer arrest at 25ºC.

Dauer formation assays

Dauer assays were performed as previously described [15]. In general, 60–80 L1s or embryos were transferred to NGM plates seeded with *E. coli* (HT115 or OP50). eCBs (final concentration 50 µM) or NMP331 (final concentration 1 µM or as indicated in Supplementary Fig. 1) were added to the bacteria immediately prior to seeding. The final concentrations of these compounds were calculated according to the volume of the NGM agar used for the preparation of the plates. Depending on the sort of essays after 3, 4 or 5 days the dauer percentage was scored. Δ7-DA was used alternatively in dauer rescue experiments at a concentration of 90nM.

Lipid Extraction and endocannabinoid analysis by HPLC-MS/MS.

The protocol is adaptation of Folch (1957) [57]. Briefly, lipid extracts were made from approximately 200 mg of frozen worm pellets grown at 20 °C. Pellets were washed with M9 buffer, then re-suspended in 1.3 ml pure methanol and sonicated three times for 30 seconds. After sonication 2.6 ml of chloroform and 1.3 ml 0.5 M KCl/0.08 M H3PO4 were added. Butylated hydroxytoluene (BHT, 0.005 % v/v) was added to prevent lipid oxidation. Samples were then sonicated for 15 min, vortexed twice for 1 min and centrifuged for 10 min at 2.000 x g to induce phase separation. The lower, hydrophobic phase was collected, dried under constant nitrogen stream, re-suspended in 100 µl of acetonitrile and loaded into dark caramel tubes using a glass pipette.

2-AG was quantified from nematode samples by liquid chromatography (Ultimate 3000 RSLC Dionex, Thermo Scientific) coupled with an ESI triple quadrupole mass spectrometer (TSQ Quantum Access Max (QQQ), Thermo-Scientific) as previously described [15].

DAF-16::GFP expression analysis

529 An stably integrated DAF-16::GFP, TJ356 was used. The expression of GFP was observed
530 using a Nikon Eclipse 800 microscope equipped with a fluorescent light source. The
531 images were captured with a Andor Clara digital camera.
532 To observe GFP distribution, 15-25 animals were mounted to an agar pad containing 20
533 mM sodium azide and analyzed immediately. No animal on the pad for more 10 min was
534 scored. DAF-16::GFP distribution was categorized based on the accumulation of GFP in
535 the nucleus or the cytoplasm (diffuse form) in the whole animal. Individual animals were
536 classified based on the presence of nuclear DAF-16::GFP in approximately 90%, 70%
537 (High translocation), 50%, 30% (Middle traslocation), 10% or none (Low Translocation)
538 of the body cells, as shown in Figure Supplementary 7**.** All the animals scored were at
539 the stage of L2 after 72 hs of growing in the second generation under free sterol
540 conditions.
541
542 **Two-electrode voltage clamp in *Xenopus oocytes*.**
543 For electrophysiological recording in *Xenopus levis* oocytes, OSM-9, OCR-2 subunits
544 subcloned into a modified pGEMHE vector were used. cRNAs were in vitro transcribed
545 from linearized plasmid DNA templates using RiboMAXTM Large Scale RNA Production
546 System (Promega, Madison, WI, USA). Xenopus oocytes were injected with 50 nl of
547 RNase-free water containing 1.0 ng of cRNA (at a 1:1 molar ratio for heteromeric
548 receptors) and maintained in Barth's solution [in mM: NaCl 88, Ca(NO3)2 0.33, CaCl2
549 0.41, KCl 1, MgSO4 0.82, NaHCO3 2.4, HEPES 10] at 18◦C. Electrophysiological recordings
550 were performed at −60 mV under two-electrode voltage-clamp with an Oocyte Clamp
551 OC-725B or C amplifier (Warner Instruments Corporation, Hamden, CT, USA).
552 Recordings were filtered at a corner frequency of 10 Hz using a 900 BT Tunable Active

553 Filter (Frequency Devices Inc., Ottawa, IL, USA). Data acquisition was performed using a
554 Patch Panel PP-50 LAB/1 interphase (Warner Instruments Corp., Hamden, CT, USA) at a
555 rate of 10 points per second. Both voltage and current electrodes were filled with 3M
556 KCl and had resistances of ~1MΩ. Data were analysed using Clampfit from the pClamp
557 6.1 software (Molecular Devices, Sunnyvale, CA). During electrophysiological recordings
558 100 µM 2-AG was added to the perfusion solution. Recording was performed at room
559 temperature and heat-stimulation (~ 36 °C) by perfusion of heated Barth's. The
560 temperature of perfused bath solutions was checked with a TC-344B temperature
561 controller (Warner Instruments) located near the oocytes. Mean ± SEM of current
562 amplitudes of responses to temperature, 100 µM 2-AG and temperature plus 100 µM 2-
563 AG in oocytes injected with either OSM-9, OCR-2 or OSM-9/OCR-2 were calculated using
564 Prism 6 software (GraphPad Software Inc., La Jolla, CA, USA).

565 **ASH calcium imaging.**

566 Animals expressing GCaMP6 in the ASH (xuEx1978 [Psra-6::Gcamp6(f), Psra-6::DsRed])
567 were immobilized in a PDMS microfluidic olfactory chip [58,59] and exposed to either a
568 control buffer or a stimulus buffer containing 100mM 2-AG (Cayman Chemical Co.
569 #62160). The required volume of 2-AG required to make 100mM solution was dissolved
570 in 0.1% ethanol before being added to S-Basal buffer. Since the 2-AG stock solution was
571 dissolved in acetonitrile, we added an equivalent volume of acetonitrile and 0.1%
572 ethanol S-basal to make the control buffer. This ensured the responses were specific to
573 2-AG. The stimulus protocol was based on previously described exposure experiments
574 [55]. Animals were allowed to acclimate in the olfactory chip for at least 5 minutes
575 before recording. Recording was performed at 10x magnification on an AxioObserver A1

inverted microscope (Zeiss) connected to a Sola SE Light Engine (Lumencor) and an ORCA-Flash 4.0 digital CMOS camera (Hamamatsu). Micromanager Software [60] was used to control image acquisition. Recording was performed at 10 frames per second and 4x4 image binning. An Arduino was used to control pinch valves to direct stimulus and control buffer to the nose of animals in the following sequence: 6 second baseline, 4 second stimulation, 10 second interstimulus interval, 4 second stimulation, 6 second washout. GCaMP fluorescence was extracted using Matlab (Mathworks) scripts and the results were plotted using GraphPad Prism.

Acknowledgments

Supported by grants of Richard Lounsbery Foundation (to D.d.M) and NIH GM1140480 (to M.J.A). Some strains were provided by the CGC, which is funded by NIH Office of Research Infrastructure Programs (P40 OD010440). We thank Sider Penkov and Teymuras Kurzchalia for sharing unpublished data, to Luisa Cochella, Cecilia Mansilla and Claudia Banchio for critically reading the manuscript and to Diego Rayes and Shawn Xu for the worm strains.

References

1. Kritchevsky SB, Kritchevsky D. Serum cholesterol and cancer risk: An Epidemiologic Perspective. Annu Rev Nutr. 1992. doi:10.1146/annurev.nu.12.070192.002135

2. Woollett LA. Where does fetal and embryonic cholesterol originate and what does it do? Annual Review of Nutrition. 2008. pp. 97–114. doi:10.1146/annurev.nutr.26.061505.111311

3. Cai J, Pajak A, Li Y, Shestov D, Davis CE, Rywik S, et al. Total cholesterol and mortality in China, Poland, Russia, and the US. Ann Epidemiol. 2004;14: 399–408. doi:10.1016/j.annepidem.2003.10.012

4. Iqbal J, Hussain MM. Intestinal lipid absorption. Am J Physiol Endo-crinol Metab. 2009;296: 1183–1194. doi:10.1152/ajpendo.90899.2008.

5. Martins IJ, Hone E, Foster JK, Sünram-Lea SI, Gnjec A, Fuller SJ, et al. Apolipoprotein E, cholesterol metabolism, diabetes, and the convergence of risk factors for Alzheimer's disease and cardiovascular disease. Molecular Psychiatry. 2006. pp. 721–736. doi:10.1038/sj.mp.4001854

6. Patel TN, Shishehbor MH, Bhatt DL. A review of high-dose statin therapy: targeting cholesterol and inflammation in atherosclerosis. Eur Heart J. 2007;28: 664–672. doi:10.1093/eurheartj/ehl445

7. Paul H A Steegmans, Durk Fekkes, Arno WHoes, Annette AA Bak, Emiel van der Does DEG. Low serum cholesterol concentration and serotonin metabolism in men. BMJ. 1996;312: 221. doi:10.1136/bmj.312.7025.221

8. Sturley SL, Patterson MC, Balch W, Liscum L. The pathophysiology and mechanisms of NP-C disease. Biochim Biophys Acta. 2004;1685: 83–7. doi:10.1016/j.bbalip.2004.08.014

9. Matyash V, Entchev E V, Mende F, Wilsch-Brauninger M, Thiele C, Schmidt AW, et al. Sterol-Derived Hormone(s) Controls Entry into Diapause in Caenorhabditis elegans by Consecutive Activation of DAF-12 and DAF-16. PLoS Biol. 2004;2: 1561–1571. doi:10.1371/journal.pbio.0020280

10. Matyash V, Geier C, Henske A, Mukherjee S, Hirsh D, Thiele C, et al. Distribution and transport of cholesterol in Caenorhabditis elegans. Mol Biol Cell. 2001;12: 1725–1736. doi:10.1091/mbc.12.6.1725

11. Motola DL, Cummins CL, Rottiers V, Sharma KK, Li T, Li Y, et al. Identification of Ligands for DAF-12 that Govern Dauer Formation and Reproduction in C. elegans. Cell. 2006;124: 1209–1223. doi:10.1016/j.cell.2006.01.037

12. Wollam J, Antebi A. Sterol Regulation of Metabolism, Homeostasis, and Development. Annu Rev Biochem. 2011;80: 885–916. doi:10.1146/annurev-biochem-081308-165917

13. Antebi A. Nuclear receptor signal transduction in C. elegans. WormBook. 2015; 1–49. doi:10.1895/wormbook.1.64.2

14. Boland S, Schmidt U, Zagoriy V, Sampaio JL, Fritsche RF, Czerwonka R, et al. Phosphorylated glycosphingolipids essential for cholesterol mobilization in Caenorhabditis elegans. Nat Chem Biol. 2017. doi:10.1038/nchembio.2347

15. Galles C, Prez GM, Penkov S, Boland S, Porta EOJ, Altabe SG, et al.

Endocannabinoids in Caenorhabditis elegans are essential for the mobilization of cholesterol from internal reserves. Sci Rep. 2018;8: 1–12. doi:10.1038/s41598-018-24925-8

16. Jie Li, Gemma Brown, Michael Ailion SL and JHT. NCR-1 and NCR-2, the C. elegans homologs of the human Niemann-Pick type C1 disease protein, function upstream of DAF-9 in the dauer formation pathways. Development. 2004;131: 5741–5752. doi:10.1242/dev.01408

17. Pastuhov SI, Matsumoto K, Hisamoto N. Endocannabinoid signaling regulates regenerative axon navigation in Caenorhabditis elegans via the GPCRs NPR-19 and NPR-32. Genes to Cells. 2016;21: 696–705. doi:10.1111/gtc.12377

18. Oakes MD, Law WJ, Clark T, Bamber BA, Komuniecki R. Cannabinoids Activate Monoaminergic Signaling to Modulate Key *C. elegans* Behaviors. J Neurosci. 2017;37: 2859–2869. doi:10.1523/JNEUROSCI.3151-16.2017

19. Chen AL, Lum KM, Lara-Gonzalez P, Ogasawara D, Cognetta AB, To A, et al. Pharmacological convergence reveals a lipid pathway that regulates C. elegans lifespan. Nat Chem Biol. 2019;15: 453–462. doi:10.1038/s41589-019-0243-4

20. Li X, Shen L, Hua T, Liu ZJ. Structural and Functional Insights into Cannabinoid Receptors. Trends Pharmacol Sci. 2020;41: 665–677. doi:10.1016/j.tips.2020.06.010

21. Hua T, Vemuri K, Nikas SP, Laprairie RB, Wu Y, Qu L, et al. Crystal structures of agonist-bound human cannabinoid receptor CB 1. Nature. 2017;547: 468–471. doi:10.1038/nature23272

663 22. Li X, Hua T, Vemuri K, Ho J, Wu Y, Wu L, et al. Crystal Structure of the Human
664 Cannabinoid Receptor CB2. Cell. 2019;176: 459–467.
665 doi:10.1016/j.cell.2018.12.011.Crystal

666 23. Muller C, Morales P, Reggio PH. Cannabinoid ligands targeting TRP channels.
667 Front Mol Neurosci. 2019;11: 1–15. doi:10.3389/fnmol.2018.00487

668 24. Tobin DM, Madsen DM, Kahn-Kirby A, Peckol EL, Moulder G, Barstead R, et al.
669 Combinatorial expression of TRPV channel proteins defines their sensory
670 functions and subcellular localization in C. elegans neurons. Neuron. 2002;35:
671 307–318. doi:10.1016/S0896-6273(02)00757-2

672 25. Bargmann CI. Chemosensation in C. elegans. WormBook. 2006; 1–29.
673 doi:10.1895/wormbook.1.123.1

674 26. Zhang S, Sokolchik I, Blanco G, Sze JY. Caenorhabditis elegans TRPV ion channel
675 regulates 5HT biosynthesis in chemosensory neurons. Development. 2004;131:
676 1629–1638. doi:10.1242/dev.01047

677 27. Oakes M, Law WJ, Komuniecki R. Cannabinoids stimulate the TRP channel-
678 dependent release of both serotonin and dopamine to modulate behavior in C.
679 elegans. J Neurosci. 2019;39: 4142–4152. doi:10.1523/JNEUROSCI.2371-18.2019

680 28. Kahn-Kirby AH, Bargmann CI. TRP channels in C. elegans. Annu Rev Physiol.
681 2006;68: 719–736. doi:10.1146/annurev.physiol.68.040204.100715

682 29. Ohnishi K, Saito S, Miura T, Ohta A, Tominaga M, Sokabe T, et al. OSM-9 and
683 OCR-2 TRPV channels are accessorial warm receptors in Caenorhabditis elegans
684 temperature acclimatisation. Sci Rep. 2020;10: 1–14. doi:10.1038/s41598-020-

75302-3

30. Benham CD, Davis JB, Randall AD. Vanilloid and TRP channels: A family of lipid-gated cation channels. Neuropharmacology. 2002;42: 873–888. doi:10.1016/S0028-3908(02)00047-3

31. Reis Rodrigues P, Kaul TK, Ho J-H, Lucanic M, Burkewitz K, Mair WB, et al. Synthetic Ligands of Cannabinoid Receptors Affect Dauer Formation in the Nematode Caenorhabditis elegans. Genes|Genomes|Genetics. 2016;6: 1695–1705. doi:10.1534/g3.116.026997

32. Ravil R. Petrova, Lindsay Knight, Shao-Rui Chen, Jim Wager-Miller, Steven W. McDaniel, Fanny Diaz, et al. Mastering tricyclic ring systems for desirable functional cannabinoid activity. Eur J Med Chem. 2013;69: 881–907. doi:doi:10.1016/j.ejmech.2013.09.038

33. Bladen C, McDaniel SW, Gadotti VM, Petrov RR, Berger ND, Diaz P, et al. Characterization of Novel Cannabinoid Based T-Type Calcium Channel Blockers with Analgesic Effects. ACS Chem Neurosci. 2014;6: 277–287. doi:10.1021/cn500206a

34. Steger KA, Shtonda BB, Thacker C, Snutch TP, Avery L. The C. elegans T-type calcium channel CCA-1 boosts neuromuscular transmission. J Exp Biol. 2005. doi:10.1242/jeb.01616

35. Magner DB, Wollam J, Shen Y, Hoppe C, Li D, Latza C, et al. The NHR-8 nuclear receptor regulates cholesterol and bile acid homeostasis in C. elegans. Cell Metab. 2013;18: 212–224. doi:10.1016/j.cmet.2013.07.007

36. Taghibiglou C, Martin HGS, Rose JK, Ivanova N, Lin CHC, Lau HL, et al. Essential role of SBP-1 activation in oxygen deprivation induced lipid accumulation and increase in body width/length ratio in Caenorhabditis elegans. FEBS Lett. 2009;583: 831–834. doi:10.1016/j.febslet.2009.01.045

37. Saifee O, Wei L, Nonet ML. The Caenorhabditis elegans unc-64 locus encodes a syntaxin that interacts genetically with synaptobrevin. Mol Biol Cell. 1998;9: 1235–1252. doi:10.1091/mbc.9.6.1235

38. Ann K, Kowalchyk JA, Loyet KM, Martin TFJ. Novel Ca2+-binding protein (CAPS) related to UNC-31 required for Ca2+-activated exocytosis. J Biol Chem. 1997;272: 19637–19640. doi:10.1074/jbc.272.32.19637

39. Ailion M, Inoue T, Weaver CI, Holdcraft RW, Thomas JH. Neurosecretory control of aging in Caenorhabditis elegans. Proc Natl Acad Sci U S A. 1999;96: 7394–7397. doi:10.1073/pnas.96.13.7394

40. Berwin B, Floor E, Martin TFJ. CAPS (Mammalian UNC-31) Protein Localizes to Membranes Involved in Dense-Core Vesicle Exocytosis. Neuron. 1998;21: 137–145. doi:10.1016/s0896-6273(00)80521-8

41. Leinwand SG, Chalasani SH. From genes to circuits and behaviors: Neuropeptides expand the coding potential of the nervous system. Worm. 2014;3: e27730. doi:10.4161/worm.27730

42. Lee BH, Ashrafi K. A TRPV channel modulates C. elegans neurosecretion, larval starvation survival, and adult lifespan. PLoS Genet. 2008;4: 1–14. doi:10.1371/journal.pgen.1000213

729 43. Yu Y, Wang L, Jiu Y, Zhan Y, Liu L, Xia Z, et al. HID-1 is a novel player in the
730 regulation of neuropeptide sorting. Biochem J. 2011;434: 383–390.
731 doi:10.1042/BJ20110027

732 44. Di Marzo V, Bifulco M, De Petrocellis L. The endocannabinoid system and its
733 therapeutic exploitation. Nat Rev Drug Discov. 2004;3: 771–784.
734 doi:10.1038/nrd1495

735 45. Cristino L, Bisogno T, Di Marzo V. Cannabinoids and the expanded
736 endocannabinoid system in neurological disorders. Nat Rev Neurol. 2020;16: 9–
737 29. doi:10.1038/s41582-019-0284-z

738 46. Clarke TL, Johnson RL, Simone JJ, Carlone RL. The endocannabinoid system and
739 invertebrate neurodevelopment and regeneration. Int J Mol Sci. 2021;22: 1–24.
740 doi:10.3390/ijms22042103

741 47. Lucanic M, Held JM, Vantipalli MC, Klang IM, Graham JB, Gibson BW, et al. N-
742 acylethanolamine signalling mediates the effect of diet on lifespan in
743 Caenorhabditis elegans. Nature. 2011;473: 226–229. doi:10.1038/nature10007

744 48. Kobayashi T, Beuchat MH, Lindsay M, Frias S, Palmiter RD, Sakuraba H, et al.
745 Late endosomal membranes rich in lysobisphosphatidic acid regulate cholesterol
746 transport. Nat Cell Biol. 1999;1: 113–118. doi:10.1038/10084

747 49. Dainese E, Oddi S, Maccarrone M. Interaction of Endocannabinoid Receptors
748 with Biological Membranes. Curr Med Chem. 2010;17: 1487–1499.
749 doi:10.2174/092986710790980087

750 50. Di Scala C, Fantini J, Yahi N, Barrantes FJ, Chahinian H. Anandamide revisited:

How cholesterol and ceramides control receptor-dependent and receptor-independent signal transmission pathways of a lipid neurotransmitter. Biomolecules. 2018;8. doi:10.3390/biom8020031

51. de Boer JF, Kuipers F, Groen AK. Cholesterol Transport Revisited: A New Turbo Mechanism to Drive Cholesterol Excretion. Trends Endocrinol Metab. 2018;29: 123–133. doi:10.1016/j.tem.2017.11.006

52. Van Voorhies WA, Ward S. Genetic and environmental conditions that increase longevity in Caenorhabditis elegans decrease metabolic rate. Proc Natl Acad Sci U S A. 1999;96: 11399–11403. doi:10.1073/pnas.96.20.11399

53. Osei-Hyiaman D, DePetrillo M, Pacher P, Liu J, Radaeva S, Bátkai S, et al. Endocannabinoid activation at hepatic CB 1 receptors stimulates fatty acid synthesis and contributes to diet-induced obesity. J Clin Invest. 2005;115: 1298–1305. doi:10.1172/JCI200523057

54. Murphy CT, Hu PJ. Insulin/insulin-like growth factor signaling in C. elegans. WormBook. 2013; 1–43. doi:10.1895/wormbook.1.164.1

55. Kahn-Kirby AH, Dantzker JLM, Apicella AJ, Schafer WR, Browse J, Bargmann CI, et al. Specific polyunsaturated fatty acids drive TRPV-dependent sensory signaling in vivo. Cell. 2004;119: 889–900. doi:10.1016/j.cell.2004.11.005

56. Brenner S. The genetics of Caenorhabditis elegans. Genetics. 1974;77: 71–94. doi:10.1093/genetics/77.1.71

57. Folch J, Lees M, Slone stanley GH. A simple method for the isolation and purification of total lipides from animal tissues. J Biol Chem. 1957;226: 497–509.

doi:10.1016/s0021-9258(18)64849-5

58. Chalasani SH, Chronis N, Tsunozaki M, Gray JM, Ramot D, Goodman MB, et al. Dissecting a circuit for olfactory behaviour in Caenorhabditis elegans. Nature. 2007;450: 63–70. doi:10.1038/nature06292

59. Chronis N, Zimmer M, Bargmann CI. Microfluidics for in vivo imaging of neuronal and behavioral activity in Caenorhabditis elegans. Nat Methods. 2007;4: 727–731. doi:10.1038/nmeth1075

60. Arthur D. Edelstein, Mark A. Tsuchida, Nenad Amodaj, Henry Pinkard, Ronald D. Vale and NS. Advanced methods of microscope control using μManager software. J Biol Methods. 2015;1: 1–18. doi:10.14440/jbm.2014.36

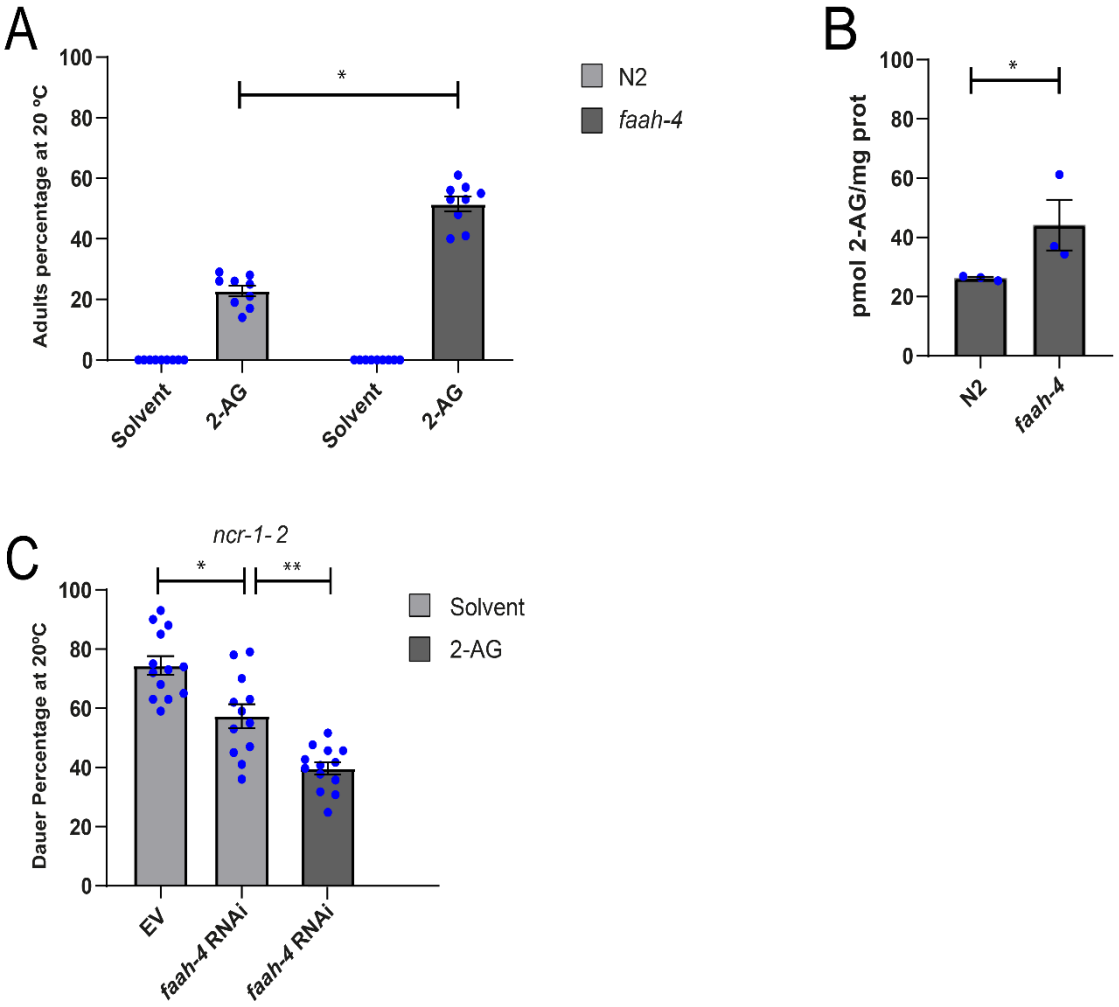

Fig 1. FAAH-4 is involved in cholesterol mobilization by 2-AG. (A) Wild type and *faah-4* animals grown for two generations in the absence of cholesterol at 20 ºC arrest as L2-like larvae. Feeding with 2-AG (50 µg/ml) increases the formation of adults in *faah-4* animals compared with N2 animals. All Pairwise Multiple Comparison Procedures (Dunn's Method), *p < 0.05. All values from n = 3 independent experiments are shown as Mean ± SEM. (B) Intracellular levels of 2-AG are elevated in *faah-4* animals. T-test, *p < 0.005. All values from n = 3 independent experiments show as Mean ± SEM. (C) *faah-4* RNAi reduces the dauer formation of strain *ncr-1-2* and enhances the ability of low concentrations of 2-AG (10 µM) to suppress the *daf-c* phenotype of these animals. All Pairwise Multiple Comparison Procedures (Holm-Sidak method), *p < 0.002, **p < 0.001. All values from n ≥ 3 independent experiments are shown as Mean ± SEM. N2 is the *C. elegans* wild-type strain.

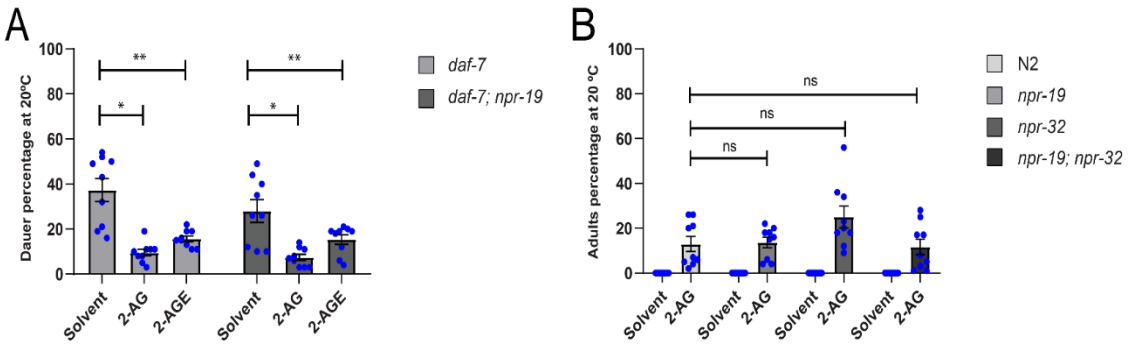

804

805 **Fig 2. Endocannabinoids stimulate transport of cholesterol by employing pathways**
806 **independent of *npr-19* and *npr-32*.** (A) Endocannabinoid suppress dauer arrest of *daf-7*
807 and *daf-7; npr-19* grown on plates containing 5 µg/ml of cholesterol. Mann-Whitney rank
808 sum test, *p < 0.001, **p < 0.001. All values from n = 3 independent experiments are
809 shown as Mean ± SEM. (B) 2-AG suppress larval arrest of *npr-19, npr-32 and npr-19; npr32*
810 animals grown for two generations on plates containing 0 µg/ml of cholesterol. All values
811 from n = 3 independent experiments show as Mean ± SEM. ns = not significant. N2 is the
812 *C. elegans* wild-type strain.

813

814

815

816

817

818

819

820

821

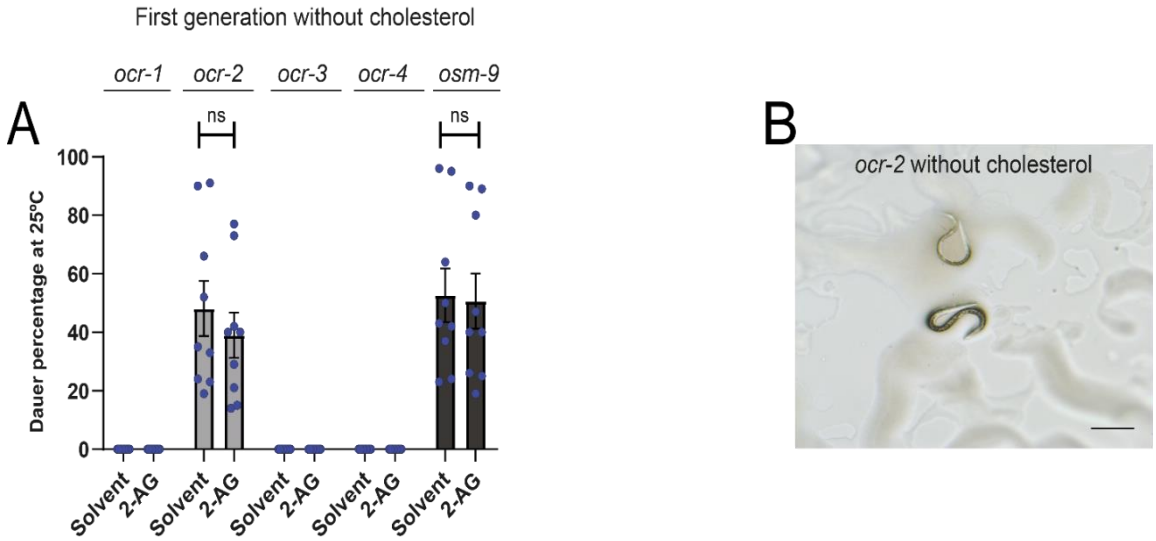

822

823 **Fig 3. *ocr-2 and osm-9* are required for 2-AG-dependent cholesterol mobilization**. (A)
824 Worms were grown in media with 0 µg/ml of cholesterol during one generation at 25 ºC.
825 All values from n = 3 independent experiments show as Mean ± SEM. ns = not significant.
826 (B) *ocr-2* undergoes dauer-like formation in the first generation when grown at 25 ºC in
827 cholesterol-free medium. The black straight line represents 0.25mm.

828

829

830

831

832

833

834

835

836

837

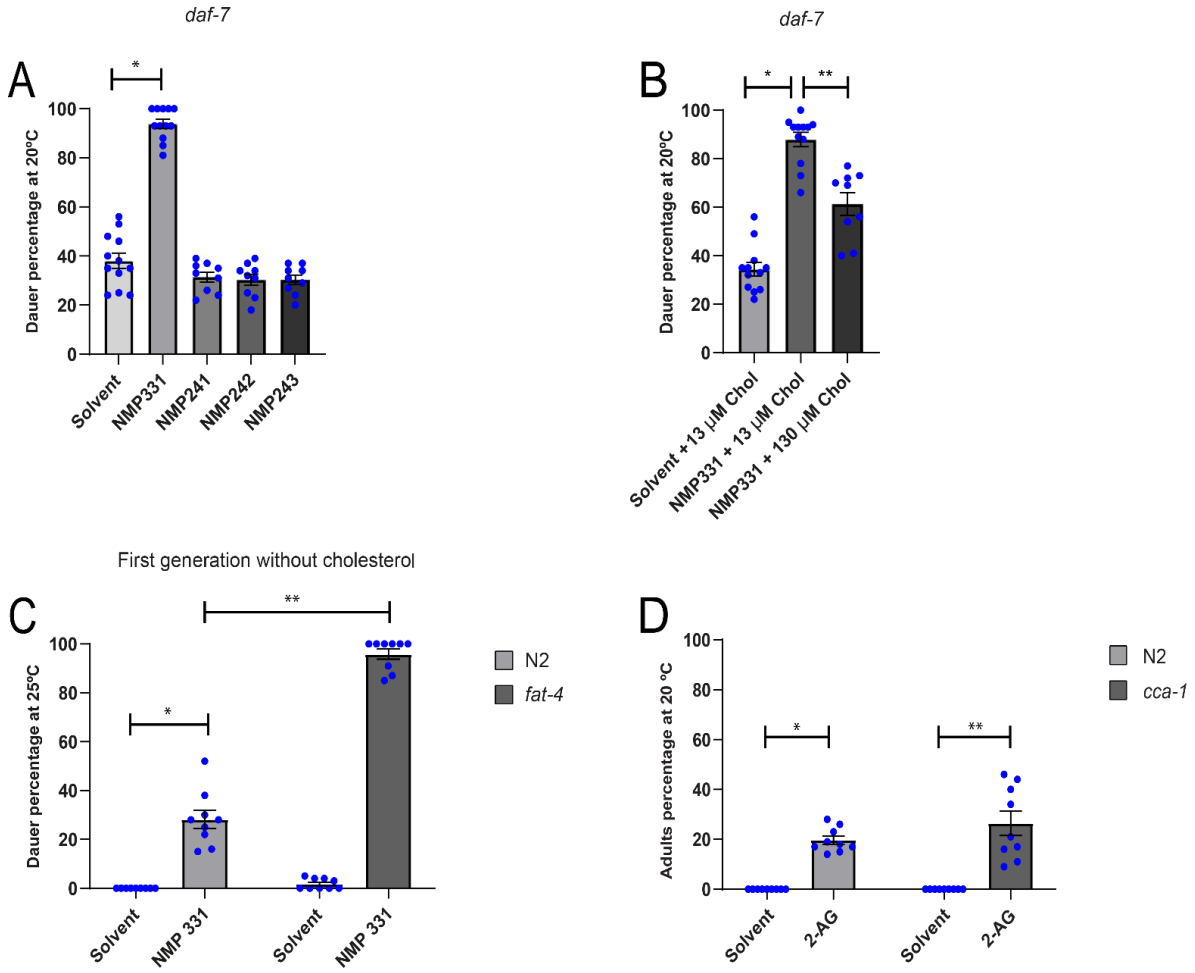

838

839 **Fig 4. The cannabinoid receptor antagonist NMP331 induces dauer formation**. (A) The
840 dauer arrest of *daf-7* worms is augmented by NMP331. All pairwise multiple comparison
841 procedures (Holm-Sidak method), *p < 0.001. All values from n ≥ 3 independent
842 experiments are shown as Mean ± SEM. (B) Dauer arrest induced by NMP331 can be
843 rescued by high cholesterol diet. All Pairwise Multiple Comparison Procedures (Holm-
844 Sidak method), *p < 0.001. **p < 0.001. All values from n ≥ 3 independent experiments
845 show as Mean ± SEM. (C) N2 and *fat-4* animals undergo a dauer arrest induced by 331
846 in the first generation when grown in cholesterol free medium. Mann-Whitney rank sum
847 test, *p < 0.001. **p < 0.005. All values from n = 3 independent experiments are show
848 as Mean ± SEM. (D) The 2-AG mediated suppression of larval arrest of N2, grown by two
849 generations in medium devoid of cholesterol, is independent of CCA-1. Mann-Whitney
850 rank sum test, *p < 0.001. t-test, **p < 0.001. All values from n = 3 independent
851 experiments show as Mean ± SEM. N2 is the *C. elegans* wild-type strain.

852

853

854

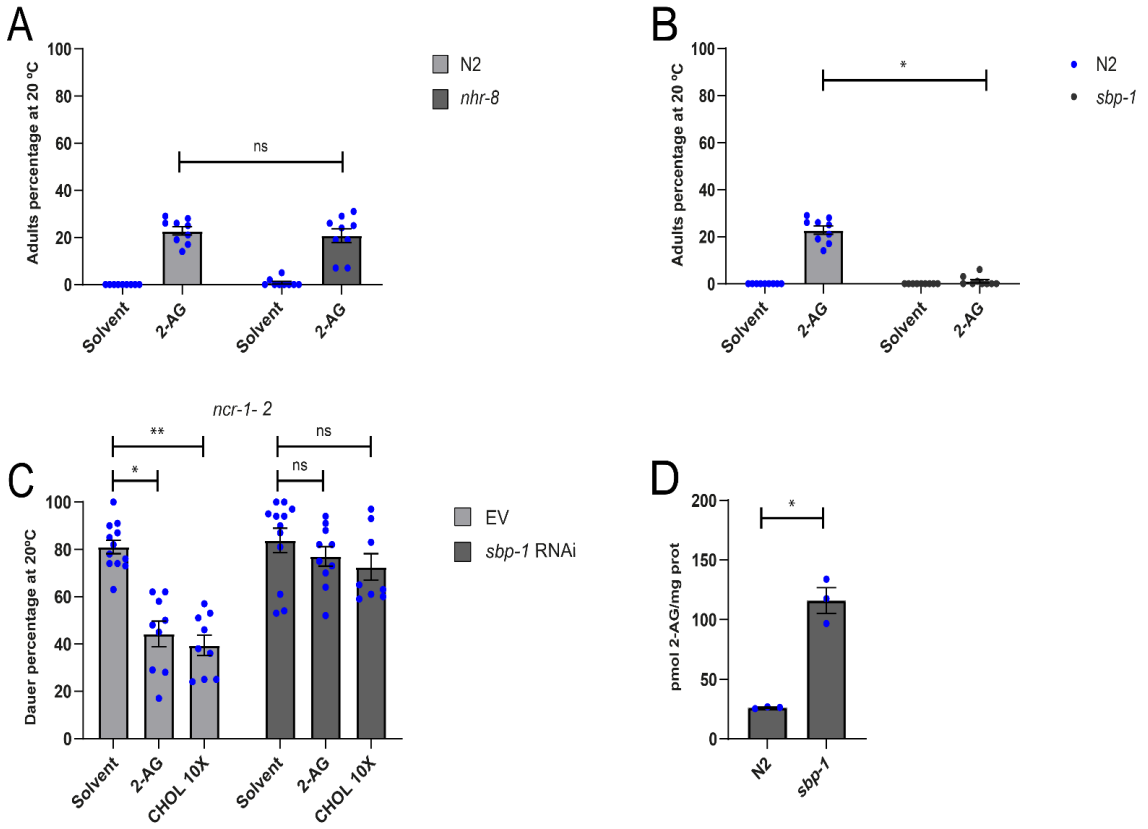

Fig 5. SBP-1 is required for 2-AG modulation of cholesterol mobilization. (A) 2-AG rescue the larval arrest of *nhr-8* worms grown two generations under 0 µg/ul of cholesterol at 20 ºC. All values from n = 3 independent experiments show as Mean ± SEM. ns = not significant. (B) 2-AG is unable to rescue the larval arrest of *sbp-1* grown two generations under 0 µg/ml of cholesterol at 20 ºC. All Pairwise Multiple Comparison Procedures (Dunn's Method), *p < 0.001. All values from n = 3 independent experiments are show as Mean ± SEM. (C) 2-AG is unable to suppress dauer formation of *a ncr-1-2* strain exposed to *sbp-1* RNAi. Kruskal-Wallis One-way analysis of variance on ranks, *p < 0.001, **p < 0.001. All values from n ≥ 3 independent experiments are show as Mean ± SEM. ns = not significant. (D) 2-AG levels are elevated in *sbp-1* animals. t-test, *p < 0.005. All values from n = 3 independent experiments are show as Mean ± SEM. N2 is the C. elegans wild-type strain.

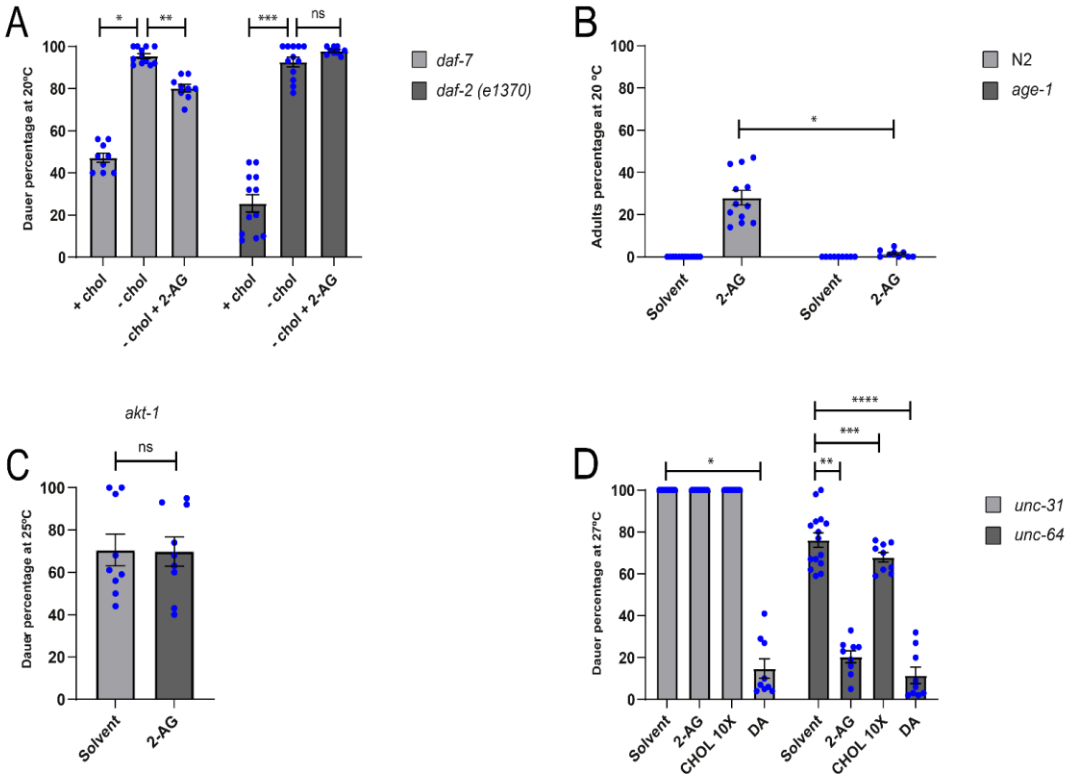

Fig 6. DAF-2 and UNC-31 are required for 2-AG-dependent cholesterol mobilization. (A) *daf-7* and *daf-2(e1370)* were grow at 20 ºC either on cholesterol or in a sterol-free media during one generation. When indicated the media was supplemented with either cholesterol 13 µM or 2-AG 50 µM. All Pairwise Multiple Comparison Procedures (Dunn's Method), *p < 0.05. **p < 0.05. ***p < 0.05. All values from n ≥ 3 independent experiments show as Mean ± SEM. ns = not significant. (B) N2 and *age-1* were grown for two generations in media with 0 µg/ml cholesterol at 20ºC. Mann-Whitney rank sum test, *p < 0.001. All values from n ≥ 3 independent experiments show as Mean ± SEM. (C) *akt-1* was grown in media with 0 µg/ml cholesterol during one generation at 25 ºC. All values from n = 3 independent experiments show as Mean ± SEM. ns = not significant. (D) 2-AG is unable rescue the daf-c phenotype of *unc-31* grown at 27 ºC. All Pairwise Multiple Comparison Procedures (Dunn's Method), *p < 0.05. All Pairwise Multiple Comparison Procedures (Holm-Sidak method), **p < 0.05. ***p < 0.05. ****p < 0.05. All values from n ≥ 3 independent experiments show as Mean ± SEM. N2 is the *C. elegans* wild-type strain.

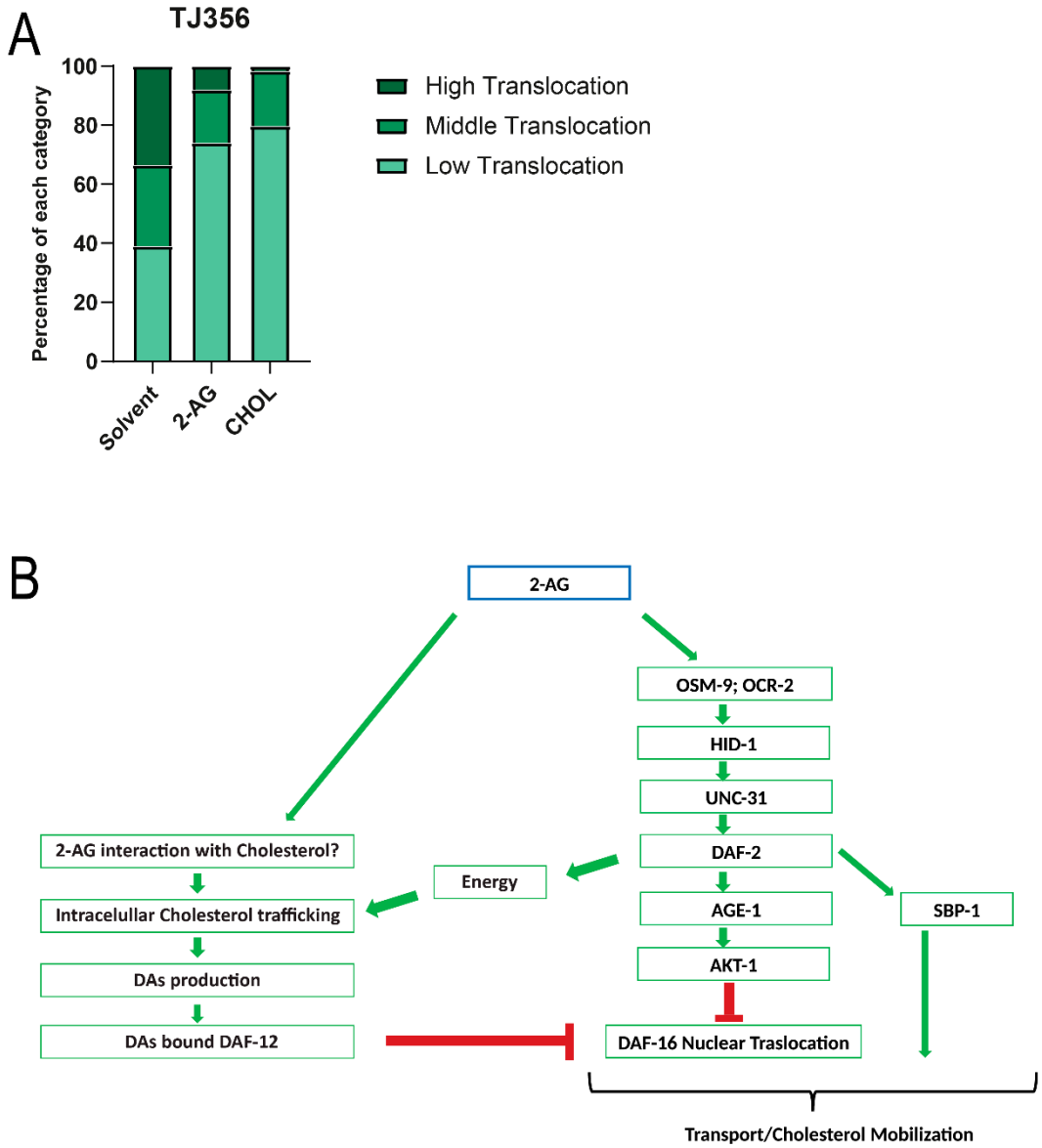

892

893 **Fig 7. 2-AG signaling inhibits nuclear translocation of DAF-16 induced by cholesterol**
894 **depletion**. (A) Nuclear translocation of DAF-16::GFP of worms grown under normal
895 cholesterol concentration (CHOL) and after cholesterol depletion for two generations
896 in the absence (solvent) or presence of 2-AG. 69 individual worms were analyzed for
897 the solvent condition, 66 for 2-AG and 64 for CHOL. (B) Working model of 2-AG
898 dependent mobilization of cholesterol. Under interaction of 2-AG with an unknown
899 target in sensory neurons, multiple signaling mechanisms are likely to converge on
900 activation of the IIS pathway and inhibition of DAF-16/FOXO. Signaling through the DAF-
901 2 insulin receptor has several functions and could be involved in modulation of the
902 intracellular traffic of cholesterol. The interaction of SBP-1 with the IIS pathway remains
903 to be established, but is likely that such interaction is essential for 2-AG-dependent
904 mobilization of cholesterol.

905

Supporting information captions

S1 Fig. TPH-1 is not required for 2-AG-dependent cholesterol mobilization. (A) N2 and *tph-1* were grown for two generations in media with 0 µg/ml cholesterol at 20ºC. Mann-Whitney rank sum test, *p < 0.001. t-test, **p < 0.001. All values from n = 3 independent experiments show as Mean ± SEM. N2 is the *C. elegans* wild-type strain.

S2 Fig. 2-AG did not elicit current in Xenopus oocytes expressing OSM-9 and OCR-2 channels. (A) Representative traces of responses (above) and temperature (below) in *Xenopus oocytes* injected with cRNAs encoding OSM-9, OCR-2, OSM-9/OCR-2. (B) Mean ± SEM of heat evoked currents. Amplitudes were calculated by measuring the differences between the peak inward currents and baseline marked with dotted lines (***p = 0.0001, n ≥ 5 per group, ANOVA followed by a Bonferroni's multi-comparison test). (C) Representative traces of responses to 100µM 2-AG either at room temperature (grey traces) or during a temperature ramp in oocytes expressing OSM-9, OCR-2 or OSM-9/OCR-2. (D) Mean ± SEM of current amplitudes of responses to temperature, 100 µM 2-AG and temperature plus 100 µM 2-AG in oocytes injected with either OSM-9, OCR-2 or OSM-9/OCR-2 (**** p < 0.0001, n ≥ 3 oocytes per group, two-way ANOVA followed by a Bonferroni multi-comparison test).

S3 Fig. ASH calcium levels are not affected by 2-AG. Calcium imaging traces of animals expressing GCaMP6 in the ASH (xuEx1978 [Psra-6::Gcamp6(f), Psra-6::DsRed]) during exposure to 2-AG. Average responses for all animals (A) are indicated by the dark blue line and the shaded area represents SEM. The same results are shown as individual traces for each animal (B). The dark grey bars indicate 4 second exposure to buffer containing 100mM 2-AG.

S4 Fig. **NMP331 induce a dauer-like formation in N2 starved for sterols and enhances dauer formation in *daf-7* mutants which can be overcome by 2-AG supplementation.** (A) N2 exhibit a dauer-like phenotype when is exposed to 1 µM NMP31 in a sterol-free medium at 25 ºC during one generation. The black straight line represents 0.25mm. (B) 2-AG antagonizes the effect of 1 µM of NMP331 in a *daf-7* worm at 20 ºC. All pairwise multiple comparison procedures (Holm-Sidak method), *p < 0.001. All values from n = 3 independent experiments show as Mean ± SEM.

S5 Fig. Mobilization of cholesterol by 2-AG is independent of the *daf-7* pathway. (A). *Daf-4* was grown at 20ºC while *daf-14* and *daf-8* were grown at 25 ºC under normal dietary cholesterol (13 µM). t-test, *p < 0.001. **p < 0.001. ***p < 0.002. All values from n = 3 independent experiments show as Mean ± SEM. (B) NMP331 does not enhances the daf-c phenotype of *daf-2* mutants. Mann-Whitney rank sum test, *p < 0.001. All values from n ≥ 3 independent experiments show as Mean ± SEM. ns = not significant.

S6 Fig. Mobilization of cholesterol by 2-AG is dependent of *hid-1.* (A) *Hid-1* is required for 2-AG dependent mobilization of cholesterol. Worms were grown at 27 ºC under normal dietary cholesterol. All pairwise multiple comparison procedures (Holm-Sidak method), *p < 0.05. All values from n = 3 independent experiments show as Mean ± SEM. ns = not significant. (B) HID-1 expression in the neurons in a *hid-1* background restores the 2-AG-dependent mobilization of cholesterol. Worms were grown at 27 ºC under normal dietary cholesterol. Mann-Whitney rank sum test, *p < 0.001. All values from n ≥ 3 independent experiments show as Mean ± SEM. ns = not significant.

S7 Fig. DAF-16::GFP nuclear translocation groups classification. Translocation categories were placed into 3 classes as the picture shows. Animals which exhibited DAF-16::GFP nuclear accumulation between 0-10% of total DAF-16::GFP were classified as Low Translocation (LowT), 30-50%, as Middle Translocation (MiddleT) and 70-90%, High Translocation (HighT). All animals shown are in a L2 larva stage.

S8 Fig. sbp-1 RNAi increases the *daf-c* phenotype of *daf-2.* *daf-2* was grown in 13 µM cholesterol at 20ºC . Mann-Whitney rank sum test, *p < 0.005. All values from n = 3 independent experiments show as Mean ± SEM.

S1 Table. Orthologues of CB1/2 grown for two generations in the absence of cholesterol arrest as L2-like larvae.

S2 Table. RNAi enhancer screen on *daf-7 (e1372)* worms. For details see text.